Thermoreversible Hydrogel for In Situ Generation and Release of HepG2 Spheroids

ARTICLE *in* BIOMACROMOLECULES · MARCH 2011

Impact Factor: 5.75 · DOI: 10.1021/bm101187b · Source: PubMed

Biomacromolecules

ARTICLE

pubs.acs.org/Biomac

Thermoreversible Hydrogel for In Situ Generation and Release of HepG2 Spheroids

Dongdong Wang, Dan Cheng, Ying Guan, and Yongjun Zhang*

Key Laboratory of Functional Polymer Materials, Institute of Polymer Chemistry, College of Chemistry, Nankai University, Tianjin 300071, China

ABSTRACT: Organ printing is an alternative to the classic scaffold-based tissue engineering approach in which functional living macrotissues and organ constructs are fabricated by assembly of the building blocks: microtissue spheroids. However, the method for scalable fabrication of cell spheroids does not exist yet. We propose here that it may be a suitable one to generate cell spheroids in thermoreversible hydrogel scaffold, followed by liquefying the scaffold and releasing the generated spheroids. We show that concentrated poly(*N*-isopropylacrylamide-*co*-acrylic acid) microgel dispersions solidify upon heating and liquefy upon cooling. A hysteresis in the cooling process was observed and explained by the slow kinetics of the dissolution of the aggregated polymer chains in the cooling process due to additional intra- and interchain interactions. Hep G2 cells are seeded by simple mixing the cells with the microgel dispersions at room temperature. Cell/scaffold constructs form in situ when heated to 37 °C. The cells proliferate and form multicellular spheroids. When brought back to room temperature, the hydrogel scaffolds liquefy, thus, releasing the generated cell spheroids. The released spheroids can attach on the cell culture plate, disassemble, and spread on the substrate, confirming the cell viability. The whole process is carried out under mild conditions and does not involve any toxic additives, which may introduce injury to the cells or DNA. It is scalable and may meet the need for large scale fabrication of cell spheroids for organ printing.

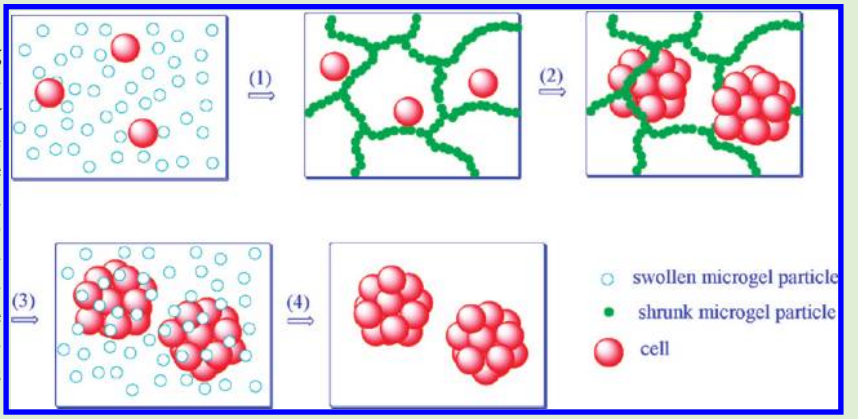

INTRODUCTION

Multicellular spheroids have long been used as in vitro three-dimensional model systems in biomedical research, such as drug screening and tumor studies.[1,2] Compared with cell monolayers, the morphology and functionality of cell spheroids are more similar to that of tissues and organs; therefore, they are able to better model the in vivo environment in which extracellular barriers and diffusion limitations pose additional obstacles to efficient and effective intracellular drug delivery.[2] In addition, they hold great promise to be used as building blocks for the construction of hybrid artificial organs.[3,4]

The classic tissue engineering approach, which uses biodegradable solid scaffold to support and guide the proliferation and differentiation of cells, still faces some limitations and challenges, such as the vascularization of thick tissue constructs. As an alternative, some researchers proposed a solid biodegradable scaffold-free approach, that is, organ printing, in which three-dimensional functional living macrotissues and organ constructs will be fabricated by "directed tissue self-assembly" of microtissue spheroids. This approach is guided by the knowledge of developmental biology and may circumvent the intrinsic limitations of the classic approach.[4]

Microtissue or multicellular spheroids are the building blocks for organ printing. For their fabrication, a lot of techniques have been developed.[1] Commonly used methods include a liquid overlay technique[5] and a hanging drop method.[2,6] They can also be generated by detaching confluent cell sheets from a planar substrate and then allowing them to aggregate and form spheroids in nonadhesive dishes.[7] Recently, Kotov et al. obtained uniform HepG2 spheroids with a narrow size distribution from hydrogel scaffolds with inverted colloidal crystal structure.[8,9] As Mironov et al.[4] pointed out, a spheroid fabrication method suitable for large-scale industrial tissue engineering and for organ printing must meet some criteria. It must be scalable, capable of standardizing the spheroid size, not inducing cell injury and DNA damage, not compromising the spheroids' capacity for sequential tissue fusion, and flexible enough to allow the generation of a diversity of tissue spheroids. A very important feature of a suitable method is its scalability. Unfortunately, most of the existing methods do not meet this criterion.[4]

Received: October 6, 2010
Revised: December 20, 2010
Published: January 19, 2011

dx.doi.org/10.1021/bm101187b | *Biomacromolecules* 2011, 12, 578–584

Scheme 1. Fabrication of Multicellular Spheroids Using Reversible Hydrogels from Thermosensitive PNIPAM Microgels[a]

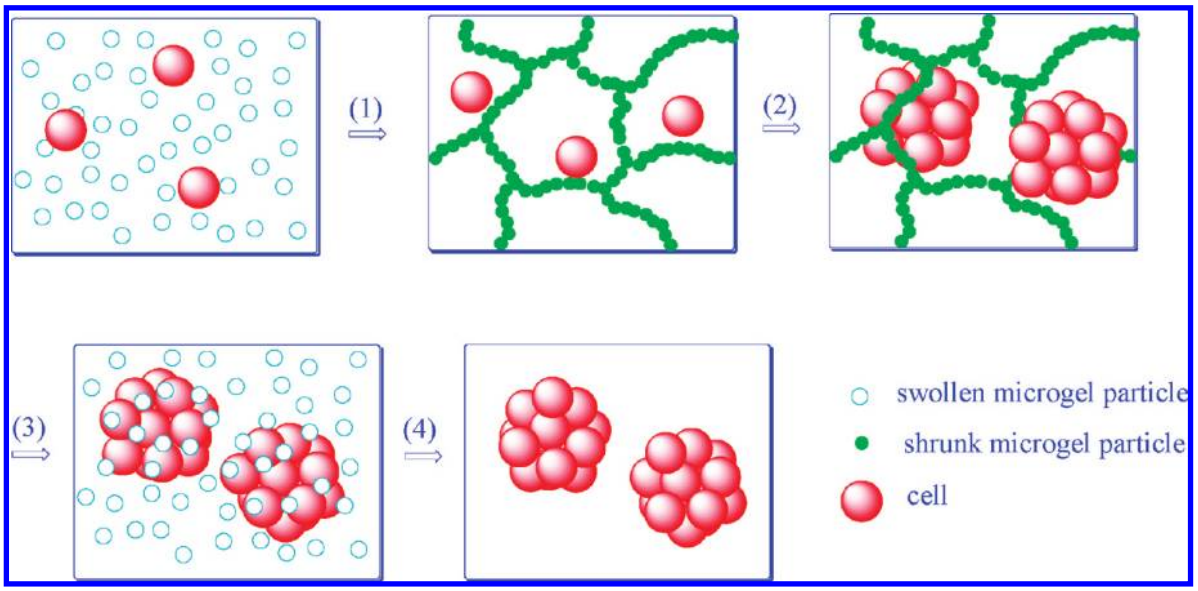

[a] (1) Cells are mixed with microgel dispersion at room temperature and heated to 37 °C to solidify the scaffold. (2) Multicellular spheroids form during culture. (3) The cell/scaffold is liquefied by cooling to room temperature. (4) Multicellular spheroids are obtained by separation from microgel particles.

Here we propose that the generation of multicellular spheroids in reversible hydrogels followed by releasing them from the scaffold may be a suitable method for large-scale spheroid fabrication. The process is schematically described in Scheme 1. Previously, several groups of researchers have shown that culturing of cells in hydrogel scaffolds will produce spheroids.[8−11] However, these hydrogels are not reversible, so the release of spheroids will be difficult. We recently developed a new in situ formed hydrogel scaffold using thermosensitive poly(*N*-isopropylacrylamide) (PNIPAM) microgel particles as building blocks.[12] HepG2 spheroids were obtained by culturing the cells in these scaffolds.[13] Thanks to its reversible properties, it is very easy not only for the scaffold to be solidified in situ (simple heating to physiological temperature), but also for its liquefaction (simple cooling to room temperature), which allows for the release and separation of cell spheroids. Previously, some authors entrapped cells in reversible hydrogels for a period of time and then released them, however, the cells did not aggregate to form spheroids.[14,15]

EXPERIMENTAL SECTION

Materials. *N*-Isopropylacrylamide (NIPAM), acrylic acid (AA), *N*, *N*′-methylenebis(acrylamide) (BIS), ammonium persulfate (APS), and sodium dodecyl sulfate (SDS) were purchased from Aldrich or Acros. AA was distilled under reduced pressure. NIPAM was recrystallized from a hexane/acetone mixture and dried in a vacuum.

Synthesis of P(NIPAM-AA) Microgels. The comonomers (NIPAM, AA, and BIS) and SDS (0.058 g, 2 mmol) were dissolved in water (95 mL). The total monomer in feed was 0.014 mol, while the molar ratio of the comonomers, $(98 - x/x/2)$ (NIPAM/AA/BIS), was varied according to the desired AA content. The mixture was transferred to a three-necked round-bottom flask equipped with a condenser and a nitrogen inlet and heated to 70 °C under a gentle stream of nitrogen. After 1 h, APS (0.068 g, dissolved in 5 mL of water) was added to initiate the reaction. The reaction was allowed to proceed for 5 h. The resultant microgels were purified by dialysis (cutoff 8000−15000 Da) against water with frequent water change for at least 1 week. The resulting microgels were denoted as PNA0.25, PNA0.50 and PNA1.00, according to the AA content, which is 0.25, 0.50, and 1.00%, respectively.

Microgel Particle Size. The size of the microgel particles were measured by dynamic light scattering on a Brookhaven 90Plus laser particle size analyzer. All the measurements were carried out at a scattering angle of 90°. The sample temperature was controlled with a build-in Peltier temperature controller.

Turbidity. The turbidity of the diluted microgel suspensions was measured on a TU-1810PC UV−vis spectrophotometer (Purkinje General, China) using water as a reference. The sample temperature was controlled with a refrigerated circulator.

Rheological Characterization. Dynamic rheological analysis of the concentrated microgel dispersions was performed on an AR2000ex rheometer (TA Instruments). Aluminum parallel plate geometry with a diameter of 40 mm was used. The sample gap was set to be 1.0 mm. The temperature was controlled by a Peltier system in the bottom plate connected with a water bath. Temperature-dependent changes in elastic (storage) modulus, G', and viscous (loss) modulus, G'', were recorded in a dynamic temperature ramp test (DTRT). All the rheological experiments were performed within the linear viscoelastic region.

Cell Culture. HepG2 cell dispersion with a concentration of 2×10^5 cells/mL was mixed with equal volume of 6 wt % microgel dispersion. To each well of a 24-well culture plate, 1 mL of the cell/microgel mixture was added. The mixtures were brought to 37 °C and gelled immediately. The cells were cultured in a media containing 90% Dulbecco's modified Eagle medium (DMEM), 10% heat-inactivated fetal calf serum, and 100 units/mL of penicillin/streptomycin. The cultures were maintained in an incubator at 37 °C with a humidified atmosphere of 5% CO_2. The medium was changed every 1−3 days.

The cell proliferation in the hydrogel scaffolds was measured using MTT assay. After cultured for a predeterminated period, the cells were incubated with 5 mL of MTT solution (5 mg/mL) for 4 h at 37 °C. After being washed with PBS three times to remove the remaining cultivating medium, 10 mL of DMSO was added to dissolve the resultant formazan crystals. The UV absorbance of the solubilized formazan crystals was measured spectrophotometrically at 490 nm to determine the number of living cells.

The appearance of the cells cultured in the scaffold was observed in situ by Olympus LX70-140 inverted fluorescence microscope at room

temperature. The samples were stained with acridine orange (AO) and ethidium bromide (EB) before imaging. The excitation wavelength used for AO was 450 ± 20 nm.

Cell Spheroid Release. After being cultured for a certain period, the cell/scaffold constructs were transferred to new culture plate. They were incubated at 25 °C for 1 h. The hydrogels gradually liquefy as the temperature was below the liquefaction temperature. The cell/microgel mixture was pipetted gently to help the release of cells and allowed to stand at 25 °C for 3 more hours to allow the cells to attach on the substrate. The liquid mixture was withdrawn, and the wells were washed with PBS three times. Culture medium of the same composition was added. The cultures were maintained in the same way as described above. The morphology of the cells was observed with an Olympus LX70-140 inverted fluorescence microscope.

RESULTS AND DISCUSSION

Sol−gel reversible hydrogels can switch between a free-flowing liquid-like state (sol phase) and a nonflowing solid-like state (gel phase), which may be triggered by external stimuli such as pH,[16] temperature,[17] or the addition of a biomolecule.[14,18] Numerous thermoreversible hydrogels have been reported in the literature.[19] Usually, these materials are random, block, or graft copolymers containing thermosensitive moieties such as PNIPAM,[17] poly(ethylene glycol-*b*-propylene glycol-*b*-ethylene glycol) (Poloxamer),[20] triblock copolymer of poly(ethylene glycol) and poly(D,L-lactic acid-*co*-glycolic acid),[21] or polyphosphazenes.[22] In contrast, here we use "spherical molecules", that is, PNIPAM microgel particles, to fabricate thermoreversible hydrogels. The sol-to-gel process, or in situ gelling, has been widely exploited for injectable drug delivery or cell immobilization.[23] Here we exploit the reverse process, that is, the gel-to-sol process, for the release of cell spheroids.

Synthesis and Characterization of P(NIPAM-AA) Microgels. As the building block of the thermoreversible hydrogel, a series of P(NIPAM-AA) microgels with various AA contents were synthesized. They were labeled as PNA0.25, PNA0.50, and PNA1.00, which has an AA content of 0.25, 0.50, and 1.00 mol %, respectively. It is well-known that PNIPAM polymer is hydrophilic and soluble in water at a temperature below its lower critical solution temperature (LCST), however, it collapses and precipitates from water when heated above its LCST.[24] The PNIPAM-based microgels are thermosensitive, too.[24] The thermosensitive behaviors of the P(NIPAM-AA) microgels were studied in 0.01 M pH 7.4 PBS by dynamic light scattering. As shown in Figure 1, upon heating, the microgel particles shrink gradually, followed by a sharp decrease in particle size. Volume phase transition temperature (VPTT), which is defined as the onset of the phase transition, was determined to be 32, 33, and 35 °C for PNA0.25, PNA0.50, and PNA1.00, respectively. VPTTs of the microgels at physiological pH and ionic strength were also measured by turbidity. As shown in Table 1, a slight decrease in VPTT was observed because water becomes poorer solvent for PNIPAM at higher ionic strength. These results are in agreement with our previous report.[13]

Sol−Gel and Gel−Sol Transitions. The thermal gelling behavior of concentrated P(NIPAM-AA) microgel dispersions was studied by dynamic rheological method. Linear viscoelastic region was first defined by stress sweep experiments. Then a dynamic temperature ramp test (DTRT) was carried out to measure the changes of dynamic moduli in the heating process. To mimic the physiological conditions, the microgel particles were dispersed in 0.01 M pH 7.4 PBS. Ionic strength was adjusted to 0.154 M by adding NaCl. As shown in Figure 2, for all three microgel dispersions, G'' dominates G' at the beginning, indicating that the dispersions are in a liquid state. Both G' and G'' first decrease with increasing temperature, which is attributed to the shrinkage of the microgel particles. The shrinking of the microgel particles results in a decreased effective volume fraction and, in turn, decreased viscosity and elastic properties.[25] As temperature continues increasing, a sharp increase in both G' and G'' was observed. As G' increases faster than G'', a crossover of G' and G'' was observed at certain temperature. Beyond this point, G' is always larger than G'', indicating the formation of a physical network.

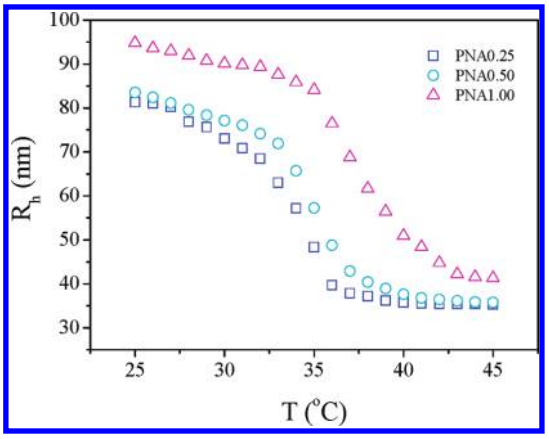

Figure 1. Hydrodynamic radii (R_h) of the P(NIPAM-AA) microgels as a function of temperature. The microgel particles are dispersed in 0.01 M pH 7.4 PBS.

Rheological properties of the in situ-formed hydrogels in a cooling process were also studied. As shown in Figure 2, when cooled to certain temperature, both G' and G'' decrease sharply. As G' decreases faster than G'', G' and G'' crossover again. Beyond this point, G' is always smaller than G'', indicating the hydrogels return to a liquid state.

The temperature where G' and G'' crossover during the heating process is defined as the gelation temperature (T_g). Similarly, the temperature where G' and G'' crossover during the cooling process is defined as the liquefaction temperature (T_l). As shown in Table 1, T_g of each system is close to the corresponding VPTT of the microgel. At VPTT, the PNIPAM polymer turns from hydrophilic to hydrophobic; therefore, this result suggests that the hydrophobic interaction among the shrunk microgel particles is the main driving force for the formation of a physical network. It is interesting that T_l is 4−5° lower than the corresponding T_g. For example, during the heating process, the sol−gel transition of the PNA0.25 microgel dispersion occurs at ∼30.5 °C, which is ∼0.5° lower than its VPTT at the same pH and ionic strength. However, during the cooling process, the reverse process, that is, the gel−sol transition, occurs at 26.5 °C, which is ∼4.5° lower than the corresponding VPTT.

A similar phenomenon was first reported by Wu and Wang[26] in 1998 when studying the coil-to-globule and globule-to-coil transitions of individual long PNIPAM chain. They found a hysteresis in the globule-to-coil transition and attributed it to the formation of some additional intrachain structures, presumably the intrachain hydrogen bonding, in the globule state, which persist during the cooling process.[26] Later, a retardation in the cooling process versus the heating process was also observed for the association and dissolution of PNIPAM chains[27−29] and the

Table 1. Volume Phase Transition Temperature (VPTT) of the Three Microgels and the Gelation Temperature (T_g) and Liquefaction Temperature (T_l) of the Concentrated Microgel Dispersions

sample	VPTT in 0.01 M pH 7.4 PBS[a] (°C)	VPTT at pH = 7.4 and I = 0.154 M[b] (°C)	T_g (°C)	T_l (°C)
PNA0.25	32	31	30.5	26.5
PNA0.50	33	32	31.5	27.5
PNA1.00	35	33	32.5	27.5

[a] Measured by dynamic light scattering. [b] Measured by turbidity.

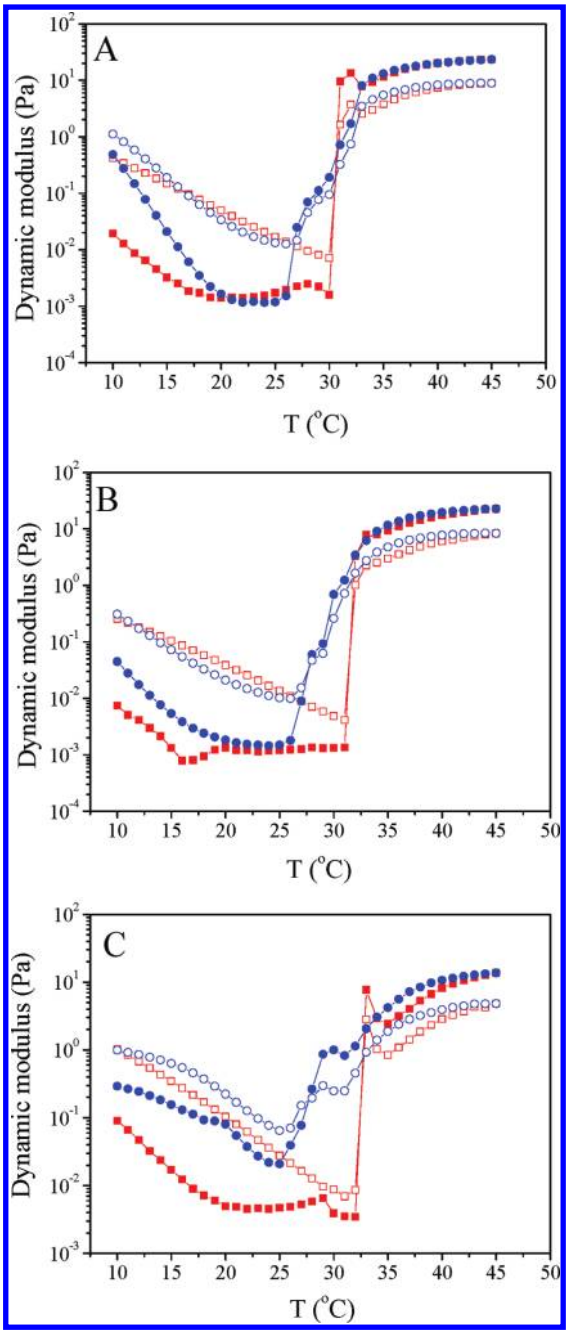

Figure 2. Evolution of dynamic moduli of the microgel dispersions (A, PNA0.25; B, PNA0.50; and C, PNA1.00) in a heating and cooling cycle under a stress of 0.1 Pa and a frequency of 0.1 Hz. Solid and open squares are for storage and loss moduli (G' and G'') during the heating process, while solid and open circles are for G' and G'' during the cooling process. Polymer concentrations are all 3.0 wt %. pH and ionic strength are 7.4 and 0.145 M, respectively.

phase transition of PNIPAM hydrogel.[30] All these phenomena were explained as follows: the aggregates formed during the heating process are further stabilized by additional intra- and interchain interactions, including hydrogen bonding and hydrophobic interaction.[31,32] Therefore, the dissolution of these aggregates in the cooling process is kinetically slow, resulting in the observed hysteresis. The formation of additional hydrogen bonds in the collapsed state during the heating process has been confirmed by FTIR studies.[28] By introducing stronger hydrogen bonding, thermosensitive polymers with very large hysteresis were designed and synthesized.[31,32] The retardation in the gel−sol process observed here can be explained in the same way. As mentioned above, the thermal gelling of the microgel dispersion results from the hydrophobic interaction among the shrunk microgel particles. In nature, this process is similar to the association of linear PNIPAM chains.[27−29] The cross-links formed during the heating process may also be stabilized by additional intra- and interchain interactions, presumably hydrogen bonding, resulting in a kinetically slow dissolution in the cooling process. As a result, a hysteresis in the gel−sol process was observed.

The morphology change of a 3.0 wt % PNA0.50 microgel dispersion in a heating/cooling cycle was visually displayed in Figure 3. Before heating, the dispersion is a liquid with a light blue color (Figure 3A). A macroscopic hydrogel was obtained when the dispersion was brought to 37 °C (Figure 3B), which shrunk to a smaller size with time (Figure 3C). When brought back to room temperature, the hydrogel liquefied gradually (Figure 3D−F). The appearance of the dispersion restored largely.

In Situ Generation and Sequential Release of HepG2 Spheroids. To demonstrate the feasibility of the application of thermal reversible hydrogel for scalable cell spheroid fabrication, we seeded HepG2 cells, the human hepatocarcinoma cell line, in the in situ-formed hydrogels to generate HepG2 cell spheroids and sequentially release them. The cells were seeded by simple mixing them with the microgel dispersions at room temperature. Then the mixtures were brought to 37 °C and solid cell/matrix construct formed in situ. We used MTT assay to determine the number of viable cells during culturing. Viable cells have the cellular reductive capacity to metabolize the yellow water-soluble tetrazolium salt, MTT, to the water-insoluble blue formazan product. Therefore, the optical density values in MTT assay represent the viable cell numbers. As shown in Figure 4, the number of viable cells increases rapidly and then levels off after cultured for 1 week. At this stage, the cell density inside the scaffold is high. Oxygen and nutrient supply by passive diffusion may not be able to meet the need of the cells any longer. These results indicate that all three hydrogels can support the proliferation of the cells very well. Interestingly, the number of viable cells in the three hydrogels increases in the order of PNA0.25 < PNA0.50 < PNA1.00. We have shown that the in situ-formed hydrogels from PNIPAM microgels shrink at 37 °C and the syneresis degree decreases with increasing AA content.[13] A reduced

Figure 3. Morphology change of a 3.0 wt % PNA0.50 microgel dispersion: (A) the original dispersion at 26 °C; (B, C) the in situ-formed hydrogel by curing the dispersion at 37 °C for 5 min (B) and 1 day (C); (D−F) return to 26 °C for 5 min (D), 10 min (E), and 3 h (F).

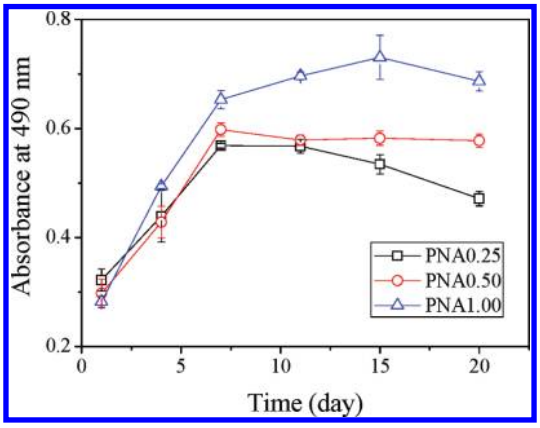

Figure 4. Proliferation of HepG2 cells cultured in the in situ-formed PNA0.25 (□), PNA0.50 (○), and PNA1.00 hydrogels (△), as assessed by MTT assays.

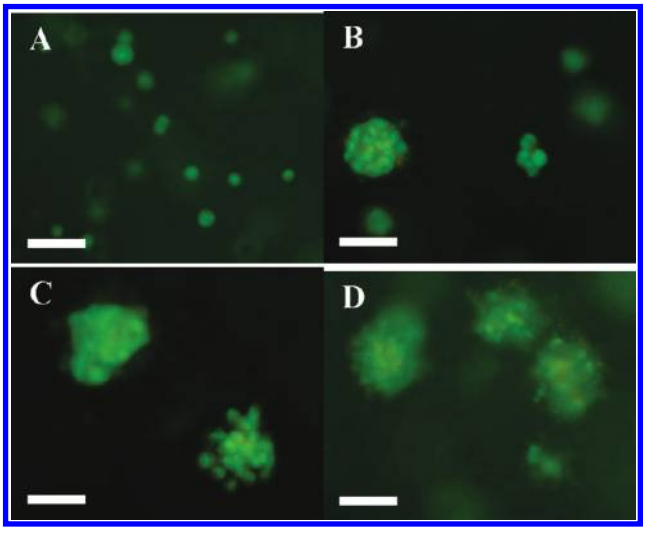

Figure 5. Fluorescence images of HepG2 cells cultured in the PNA0.50 hydrogel for 0 (A), 7 (B), 14 (C), and 21 days (D). The cells were double-stained with AO/EB. Scale bar: 100 μm.

shrinkage is beneficial for the proliferation of cells, because it is easier for the transportation of oxygen, nutrient, and also metabolic waste inside the hydrogel scaffold. Therefore, the number of viable cells increases with increasing AA content in the microgels.

The morphology of the cells cultured in the hydrogel scaffolds was studied using inverted fluorescence microscopy after stained with AO/EB. In agreement with our previous report, HepG2 spheroids form in all three hydrogels.[13] As an example, the morphology change of the cells cultured in PNA0.50 hydrogel was shown in Figure 5. At the beginning, the cells are single, round, and distributed inside the cell/scaffold construct homogenously (Figure 5A). But after being cultured for 7 days, most of the cells exist as multicellular spheroids (Figures 5B−D). The formation of HepG2 spheroids may be attributed to the relatively weak cell−substrate interaction.[8] Therefore, the cells tend to aggregate via cell−cell interaction instead of attaching to the hydrogel walls.

To release the in situ generated cell spheroids, the cell/scaffold constructs were cooled back to room temperature. As the hydrogel scaffold liquefies, spatial constraint from the solid scaffold is removed. The released cell spheroids can be easily collected by centrifugation. This mild process should not result in any cell injury or DNA damage. To further study their viability, the released spheroids were allowed to attach on the surface of the 2D tissue culture plate. Their disassembly and spreading behavior was studied.

Figure 6A shows the cell spheroids attached on the 2D substrate. It was known that HepG2 cells are adherent; therefore, the released spheroids tend to attach on solid substrate. As shown in Figures 6B−D, the spheroids gradually disassemble and spread on the substrate. The cells attached on the substrate present an irregular shape with protrusions, which is very different from the cells cultured in the 3D hydrogel scaffolds. The spreading of HepG2 spheroids was first reported by Purcell et al. and exploited as a simple and useful end point to examine the in vitro "acute" cytotoxicity of a test compound to compare relative toxicity among different test agents.[33] They suggested the cell spreading may be the result of cell division and immigration from inside spheroids. Kotov et al.[8] also reported the spreading of Hep G2 spheroids on 2D culture substrate, which were removed from a hydrogel scaffold on purpose. As for the mechanism of the disassembly of the spheroids, the strong interaction between the

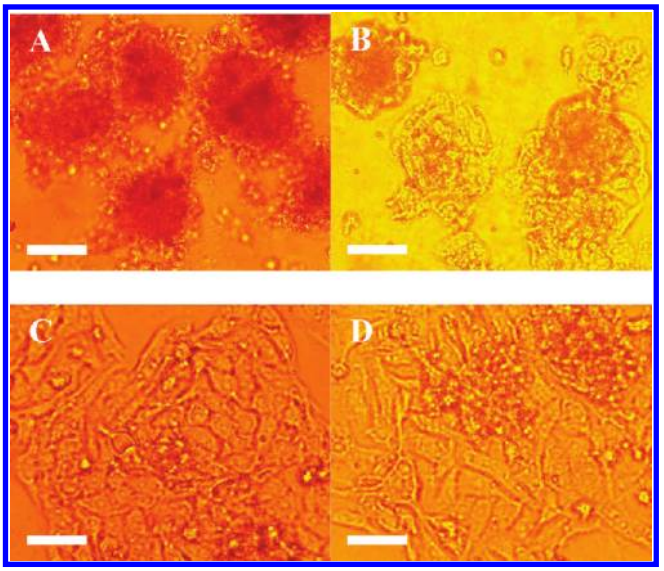

Figure 6. Attachment and disassembly of the released spheroids on the surface of 2D tissue culture plate. The cell spheroids were cultured on 2D substrate for 0 h (A), 4 h (B), 1 day (C), and 3 days (D), respectively. Before release, the HepG2 cells have been cultured in PNA0.50 hydrogel for 21 days. Scale bar: 100 μm.

cells and the substrate may be considered as the driving force. Because the prevention of cell−substrate interactions is the key to promote cell−cell interactions and thus allow the aggregation of cells, it is reasonable to expect that the introduction of cell−substrate interactions will result in the disassembly of cell spheroids. The ability to disassemble and spread confirms the viability of the spheroids.[8,33] In particular, these results indicate that the cells residing in the inner part of the spheroids are not only alive, but also retain the capability to migrate.[8] The disassembly and spreading of the spheroids also hint that the released spheroids may have the ability to fuse with other spheroids under proper conditions, which is crucial for their application in organ printing.

CONCLUSIONS

We presented here that thermoreversible hydrogels may be used for the fabrication of multicellular spheroids, which are the building blocks for further assembly to produce functional tissues or organs using the organ printing approach. We showed that under proper conditions the PNIPAM microgel dispersions solidify by simple heating to 37 °C, and they return to be liquid when cooled back to room temperature. Hep G2 cells were seeded and cultured inside the in situ-formed hydrogels. They form multicellular spheroids because of the weak cell−substrate interactions. The resultant spheroids were released by simple cooling to room temperature. The materials used here are totally synthesized polymers and free from any biological contamination. No additive or harsh conditions, which may induce injury to cell or DNA, are used. More importantly, the process is scalable, thus, may meet the requirement for large scale fabrication of cell spheroids. Efforts are still needed to improve the control over the size and structure of the cell spheroids.

AUTHOR INFORMATION

Corresponding Author

*E-mail: yongjunzhang@nankai.edu.cn.

ACKNOWLEDGMENT

We thank financial support for this work from the Ministry of Science and Technology of China (Grant No. 2007DFA50760), the National Natural Science Foundation of China (Grant Nos. 20974049 and 20974050), Tianjin Committee of Science and Technology (10JCYBJC02000), and the Key Laboratory of Polymer Chemistry and Physics of Ministry of Education, Peking University, China.

REFERENCES

(1) Lin, R. Z.; Chang, H. Y. *Biotechnol. J.* **2008**, *3*, 1172–1184.
(2) Ho, V.; Muller, K. H.; Barcza, A.; Chen, R. J.; Slater, N. *Biomaterials* **2010**, *31*, 3095–3102.
(3) Mironov, V.; Kasyanov, V.; Drake, C.; Markwald, R. R. *Regen. Med.* **2008**, *3*, 93–103.
(4) Mironov, V.; Visconti, R. P.; Kasyanov, V.; Forgacs, G.; Drake, C. J.; Markwald, R. R. *Biomaterials* **2009**, *30*, 2164–2174.
(5) Yuhas, J. M.; Li, A. P.; Martinez, A. O.; Ladman, A. J. *Cancer Res.* **1977**, *37*, 3639–3643.
(6) Bartosh, T. J.; Ylöstalo, J. H.; Mohammadipoor, A.; Bazhanov, N.; Coble, K.; Claypool, K.; Lee, R. H.; Choi, H.; Prockop, D. J. *Proc. Natl. Acad. Sci. U.S.A.* **2010**, *107*, 13724–13729.
(7) Cooperstein, M. A.; Canavan, H. E. *Langmuir* **2010**, *26*, 7695–7707.
(8) Lee, J.; Cuddihy, M. J.; Cater, G. M.; Kotov, N. A. *Biomaterials* **2009**, *30*, 4687–4694.
(9) Zhang, Y.; Wang, S. P.; Eghtedari, M.; Motamedi, M.; Kotov, N. A. *Adv. Funct. Mater.* **2005**, *15*, 725–731.
(10) Yang, J.; Goto, M.; Ise, H.; Cho, C. S.; Akaike, T. *Biomaterials* **2002**, *23*, 471–479.
(11) Underhill, G. H.; Chen, A. A.; Albrecht, D. R.; Bhatia, S. N. *Biomaterials* **2007**, *28*, 256–270.
(12) Gan, T.; Zhang, Y.; Guan, Y. *Biomacromolecules* **2009**, *10*, 1410–1415.
(13) Gan, T.; Guan, Y.; Zhang, Y. *J. Mater. Chem.* **2010**, *20*, 5937–5944.
(14) Konno, T.; Ishihara, K. *Biomaterials* **2007**, *28*, 1770–1777.
(15) Chen, T. H.; Small, D. A.; McDermott, M. K.; Bentley, W. E.; Payne, G. F. *Biomacromolecules* **2003**, *4*, 1558–1563.
(16) Lee, S. Y.; Lee, Y.; Kim, J. E.; Park, T. G.; Ahn, C. *J. Mater. Chem.* **2009**, *19*, 8198–8201.
(17) Hu, J.; Ge, Z.; Zhou, Y.; Zhang, Y.; Liu, S. *Macromolecules* **2010**, *43*, 5184–5187.
(18) Shu, X. Z.; Liu, Y. C.; Luo, Y.; Roberts, M. C.; Prestwich, G. D. *Biomacromolecules* **2002**, *3*, 1304–1311.
(19) Jeong, B.; Kim, S. W.; Bae, Y. H. *Adv. Drug Delivery Rev.* **2002**, *54*, 37–51.
(20) Lee, Y.; Chung, H. J.; Yeo, S.; Ahn, C. H.; Lee, H.; Messersmith, P. B.; Park, T. G. *Soft Matter* **2010**, *6*, 977–983.
(21) Yu, L.; Chang, G. T.; Zhang, H.; Ding, J. D. *J. Polym. Sci., Polym. Chem.* **2007**, *45*, 1122–1133.
(22) Lee, B. H.; Lee, Y. M.; Sohn, Y. S.; Song, S. C. *Macromolecules* **2002**, *35*, 3876–3879.
(23) Jeong, B.; Lee, K. M.; Gutowska, A.; An, Y. H. H. *Biomacromolecules* **2002**, *3*, 865–868.
(24) Pelton, R. *Adv. Colloid Interface Sci.* **2000**, *85*, 1–33.
(25) Senff, H.; Richtering, W. *J. Chem. Phys.* **1999**, *111*, 1705–1711.
(26) Wu, C.; Wang, X. *Phys. Rev. Lett.* **1998**, *80*, 4092–4094.
(27) Ding, Y. W.; Ye, X. D.; Zhang, G. Z. *Macromolecules* **2005**, *38*, 904–908.
(28) Cheng, H.; Shen, L.; Wu, C. *Macromolecules* **2006**, *39*, 2325–2329.
(29) Tang, Y. C.; Ding, Y. W.; Zhang, G. Z. *J. Phys. Chem. B* **2008**, *112*, 8447–8451.
(30) Sun, S. T.; Hu, J.; Tang, H.; Wu, P. Y. *J. Phys. Chem. B* **2010**, *114*, 9761–9770.

(31) Mori, T.; Beppu, S.; Berber, M. R.; Mori, H.; Makimura, T.; Tsukamoto, A.; Minagawa, K.; Hirano, T.; Tanaka, M.; Niidome, T.; Katayama, Y.; Hirano, T.; Maeda, Y. *Langmuir* **2010**, *26*, 9224–9232.
(32) Berber, M. R.; Mori, H.; Hafez, I. H.; Minagawa, K.; Tanaka, M.; Niidome, T.; Katayama, Y.; Maruyama, A.; Hirano, T.; Maeda, Y.; Mori, T. *J. Phys. Chem. B* **2010**, *114*, 7784–7790.
(33) Xu, J. S.; Ma, M. W.; Purcell, W. M. *Toxicol. Appl. Pharmacol.* **2003**, *189*, 112–119.